


Original Research

# Cerebellar remodelling decades after spinal cord insult: neuroplasticity in poliomyelitis survivors

Stacey Li Hi Shing<sup>1</sup>, Aizuri Murad<sup>1</sup>, Jasmin Lope<sup>1</sup>, Orla Hardiman<sup>1</sup>, Peter Bede<sup>1,2,\*</sup> 

<sup>1</sup>Computational Neuroimaging Group, Trinity College Dublin, D02 PN40 Dublin, Ireland

<sup>2</sup>Pitié-Salpêtrière University Hospital, Sorbonne University, 53400 Paris, France

\*Correspondence: [bedep@tcd.ie](mailto:bedep@tcd.ie) (Peter Bede)

Academic Editor: Foteini Christidi

Submitted: 1 September 2021 Revised: 15 September 2021 Accepted: 22 September 2021 Published: 23 March 2022

## Abstract

**Background:** The cerebellum integrates a multitude of motor and cognitive processes through ample spinal and supratentorial projections. Despite emerging evidence of adaptive neuroplasticity, cerebellar reorganisation in response to severe spinal insult early in life is poorly characterised. The objective of this study is the systematic characterisation of cerebellar integrity metrics in a cohort of adult poliomyelitis survivors as a template condition for longstanding lower motor neuron injury. **Methods:** A total of 143 participants, comprising 43 adult poliomyelitis survivors and 100 age- and sex-matched healthy controls were recruited in a prospective, single-centre neuroimaging study with a uniform structural and diffusion imaging protocol. First, standard voxelwise grey and white matter analyses were performed. Then, the cerebellum was anatomically segmented into lobules, and cortical thickness and grey matter volumes were evaluated in each lobule. The integrity of cerebellar peduncles was also assessed based on their diffusivity profiles. **Results:** Compared to healthy controls, poliomyelitis survivors exhibited greater cortical thickness in lobules I, II, and III in the right hemisphere and in lobules VIIIA and VIIIB bilaterally. A trend of higher cortical thickness was also detected lobules I, II and III in the left hemisphere. Enhanced cerebellar peduncle organisation was detected, particularly within the middle cerebellar peduncles. **Conclusions:** Increased cerebellar integrity measures in poliomyelitis survivors are primarily identified in lobules associated with sensorimotor functions. The identified pattern of cerebellar reorganisation may represent compensatory changes in response to severe lower motor neuron injury in childhood and ensuing motor disability.

**Keywords:** Neuroplasticity; Cerebellum; Poliomyelitis; Motor neuron disease; Magnetic resonance imaging; Neuroimaging

## 1. Introduction

Poliomyelitis reached epidemic proportions in the early 20th century and is still endemic today in some parts of Asia [1]. It predominantly affected young children under the age of five, induced asymmetrical flaccid paralysis and carried a mortality rate of 5–10% owing to respiratory failure and vasomotor complications [2]. Today, there is an estimated 15–20 million polio survivors across the globe who are living with the lasting effects of the original infection [3], of which 20–85% meet the March of Dimes criteria for post-polio syndrome (PPS) [4,5]. The ‘late effects of polio’ (LEoP) is a broad term that refers to new symptoms due to motor-unit dysfunction or biomechanical sequelae from polio-related surgeries, musculoskeletal deformities and long-term muscle weakness and atrophy [6]. The term post-polio syndrome (PPS) denotes persistent and progressive motor decline, but other symptoms such as generalised fatigue, chronic pain, cold intolerance, sleep disturbances, neuropsychological deficits and sensory impairments are also recognised features [3,7].

Despite a predilection for the spinal anterior horns, supraspinal involvement, including cerebellar pathology, has been described in the literature. Previous post-mortem studies revealed polio-induced lesions affecting subcortical

regions such as the substantia reticularis [8–10], putamen, caudate, locus coeruleus, substantia nigra [9], vestibular nuclei [10,11], hypothalamus and thalamus [8,9,12,13]. Reports of cortical involvement are inconsistent; it is thought to be limited to motor and pre-motor areas [9] and the cerebellar pathology limited to the vermis and deep cerebellar nuclei. Accounts of involvement of cerebellar cortical layers are strikingly conflicting [9,10,14,15]. Sporadic cerebellar manifestations, such as ataxia, nystagmus, vertigo and intention tremor had been linked to poliovirus type 1 [16–18]. The rarity of frank cerebellar findings was hypothesised to be due to limited cerebellar degeneration and the challenge of ascertaining cerebellar signs in the presence of widespread lower motor neuron degeneration [15]. More recent functional [19,20] and structural [21] studies speculate that supraspinal alterations may represent adaptive processes in response to longstanding lower motor neuron loss.

The cerebellum is implicated in a multitude of motor and cognitive functions spanning from motor control, coordination, maintenance of balance, posture, motor learning, to higher cognitive and affective regulatory processes [22]. Each cerebellar hemisphere can be subdivided into 3 lobes and further delineated into 10 smaller lobules (I–X); anterior lobe (lobules I–V), posterior lobe (lobules VI–



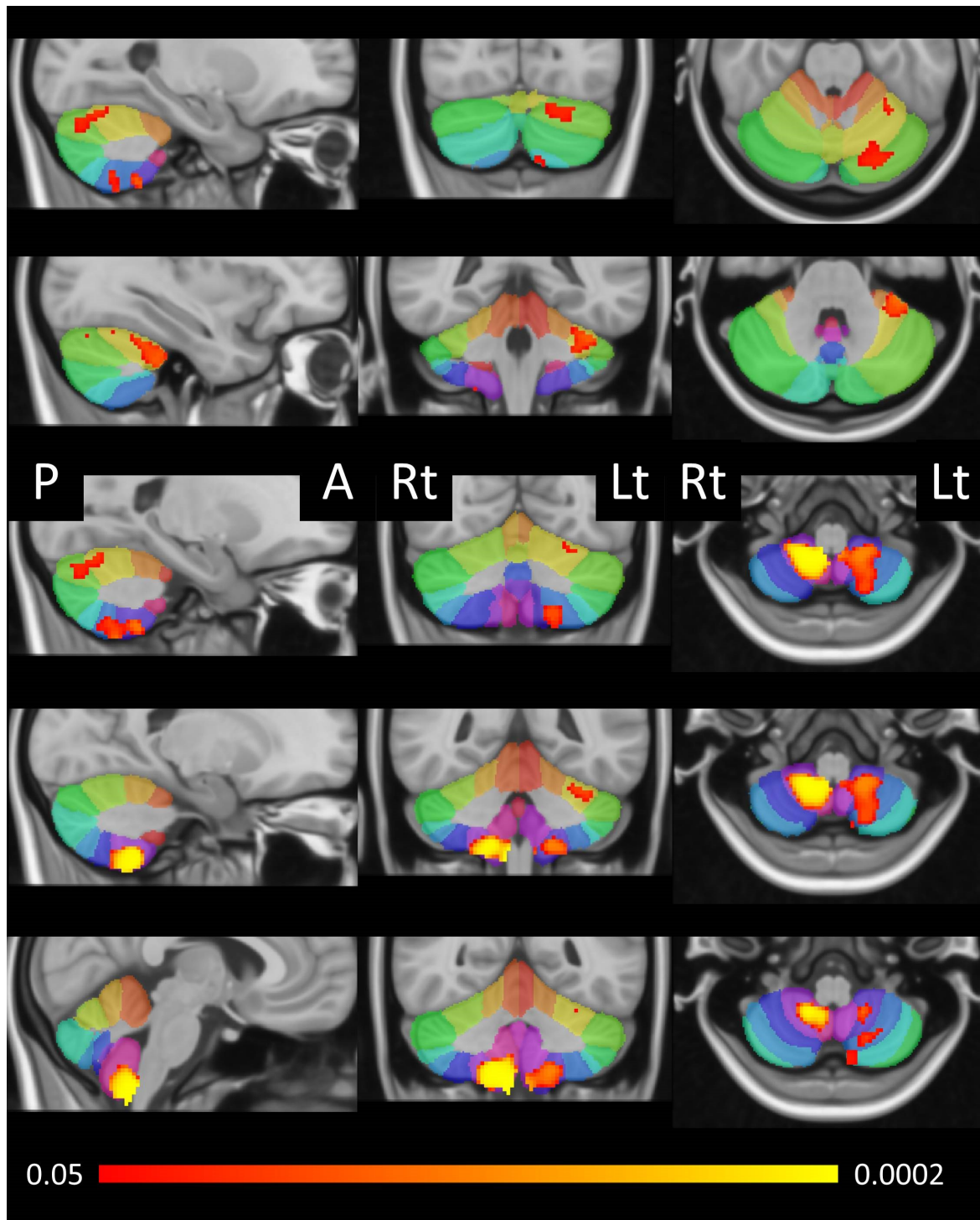


**Fig. 1. Morphometric patterns of increased cerebellar grey matter partial volumes in poliomyelitis survivors indicated in red-yellow at  $p < 0.05$  FWE TFCE corrected for age, gender and total intracranial volumes (TIV).** The labels of the Diedrichsen probabilistic cerebellar atlas are shown as underlay to aid localisation. Radiological convention is used, first column presents sagittal views, second column shows coronal views and last column depicts axial views. Lt, Left; Rt, Right; A, Anterior; P, Posterior.

IX) and flocculonodular lobe (lobule X) [23]. The grey matter of the cerebellar cortex is arranged into three layers (from outer to inner; molecular, Purkinje and granular) which contains both excitatory and inhibitory neurons integrating cerebellar inputs and modulating cerebellar outputs.

Deeply embedded within the cerebellar white matter are the deep cerebellar nuclei (dentate, emboliform, globose and fastigial) which are the sole output structures of the cerebellum. Climbing fibres, originating from the contralateral inferior olivary nucleus, and mossy fibres, largely via the

**Table 1. The demographic profile of study participants.**

	Healthy controls (n = 100)	Poliomyelitis survivors (n = 43)	<i>p</i> value
Age (years), mean (SD)	66.13 (6.472)	66.14 (6.707)	0.994
Gender (male)	52 (52%)	18 (41.9%)	0.266
Age at acute poliomyelitis (years), mean (SD)	-	2.60 (2.991)	-
ALSFRS-r total (max. 48), mean (SD)	-	39.65 (7.368)	-

SD, standard deviation.

pontocerebellar tract, are the two main input routes to the cerebellar cortex and provide excitatory signals to Purkinje fibres. Functionally, the cerebellum has been suggested to be topographically organised. The ‘motor cerebellum’ is thought to primarily include the anterior lobe and lobule VIII of posterior lobe. Lobules VI and VII constitute the ‘cognitive cerebellum’ and posterior vermis is generally regarded as the ‘limbic cerebellum’ [23,24].

The majority of quantitative imaging studies in motor neuron diseases focus either on amyotrophic lateral sclerosis [25,26] or on primary lateral sclerosis [27,28]. Cerebellar degeneration in motor neuron disorders has been linked to a multitude of manifestations including eye-movement abnormalities, bulbar dysfunction, pseudobulbar affect and deficits in social cognition [29–34]. Cerebral studies of lower motor neuron predominant conditions and in poliomyelitis survivors are scarce. With the striking paucity of neuroimaging studies and conflicting accounts of cerebellar involvement in poliomyelitis survivors, our primary objective is the comprehensive, multiparametric characterisation of cerebellar involvement *in vivo*. An additional aim of our study is the evaluation of cerebro-cerebellar connectivity via the targeted assessment of cerebellar peduncles. Based on recent studies of long-term poliomyelitis survivors, we hypothesize that focal cerebellar changes may be detected confined to lobules that mediate sensorimotor processes instead of global cerebellar degeneration.

## 2. Methods

### 2.1 Ethics statement

The study was approved by the institutional ethics committee (Beaumont Hospital, Dublin Ireland) and all participants provided written informed consent.

### 2.2 Participants

Forty-three adult poliomyelitis survivors and 100 healthy controls (HC) enrolled in a prospective, cross-sectional neuroimaging study. All participating adult poliomyelitis survivors had a verified diagnosis of poliomyelitis in infancy/childhood supported by clinical and electromyographic findings. Inclusion criteria included the ability to tolerate the duration of MR imaging and exclusion criteria included comorbid neuro-inflammatory, neurovascular, neoplastic, psychiatric conditions or prior head or spinal cord injuries. Healthy controls were unrelated to

participating patients and had no known neurological diagnoses or previous head injury. Demographic and clinical details were carefully recorded for polio survivors including age at acute poliomyelitis infection. Functional disability was appraised using the revised ALS rating scale (ALSFRS-r) [35]. The age profiles of the two groups were contrasted by ANOVA and chi-squared test was utilised for the comparison of sex ratios in controls and poliomyelitis survivors.

### 2.3 Magnetic resonance imaging

MRI data were acquired on a 3 Tesla Philips Achieva Magnetic resonance (MR) platform. A 3D Inversion Recovery prepared Spoiled Gradient Recalled echo (IR-SPGR) sequence was implemented to acquire T1-weighted (T1w) images with the following parameters; spatial resolution of  $1 \times 1 \times 1$  mm, field-of-view (FOV) of  $256 \times 256 \times 160$  mm, flip angle =  $8^\circ$ , SENSE factor = 1.5, TR/TE = 8.5/3.9 ms, TI = 1060 ms. A spin-echo echo planar imaging (SE-EPI) pulse sequence was used to acquire diffusion tensor images (DTI) with a 32-direction Stejskal-Tanner diffusion encoding scheme; 60 slices without interslice gaps, FOV =  $245 \times 245 \times 150$  mm, TR/TE = 7639/59 ms, SENSE factor = 2.5, b-values = 0, 1100 s/mm<sup>2</sup>, dynamic stabilisation and spectral presaturation with inversion recovery (SPIR) fat suppression. FLAIR images were reviewed to assess for comorbid inflammatory and vascular. FLAIR images were acquired in axial orientation using an Inversion Recovery Turbo Spin Echo (IR-TSE) sequence: spatial resolution =  $0.65 \times 0.87 \times 4$  mm, 30 slices with 1 mm gap, FOV =  $230 \times 183 \times 150$  mm, TR/TE = 11000/125 ms, TI = 2800 ms,  $120^\circ$  refocusing pulse, with flow compensation and motion smoothing and a saturation slab covering the neck region.

### 2.4 Cortical thickness and volume analyses

A validated segmentation algorithm [21] was implemented to estimate cerebellar cortical thickness and lobular volumes. Pre-processing steps included the ‘denoising’ of raw structural data in native space, inhomogeneity corrections, affine registration to the Montreal Neurological Institute (MNI) space, inhomogeneity corrections in MNI space, cerebellar cropping, low dimensional non-linear registration estimation, and intensity normalization. Cerebellar volume metrics were generated for each lobule using a patch-based segmentation algorithm [22] separately in the

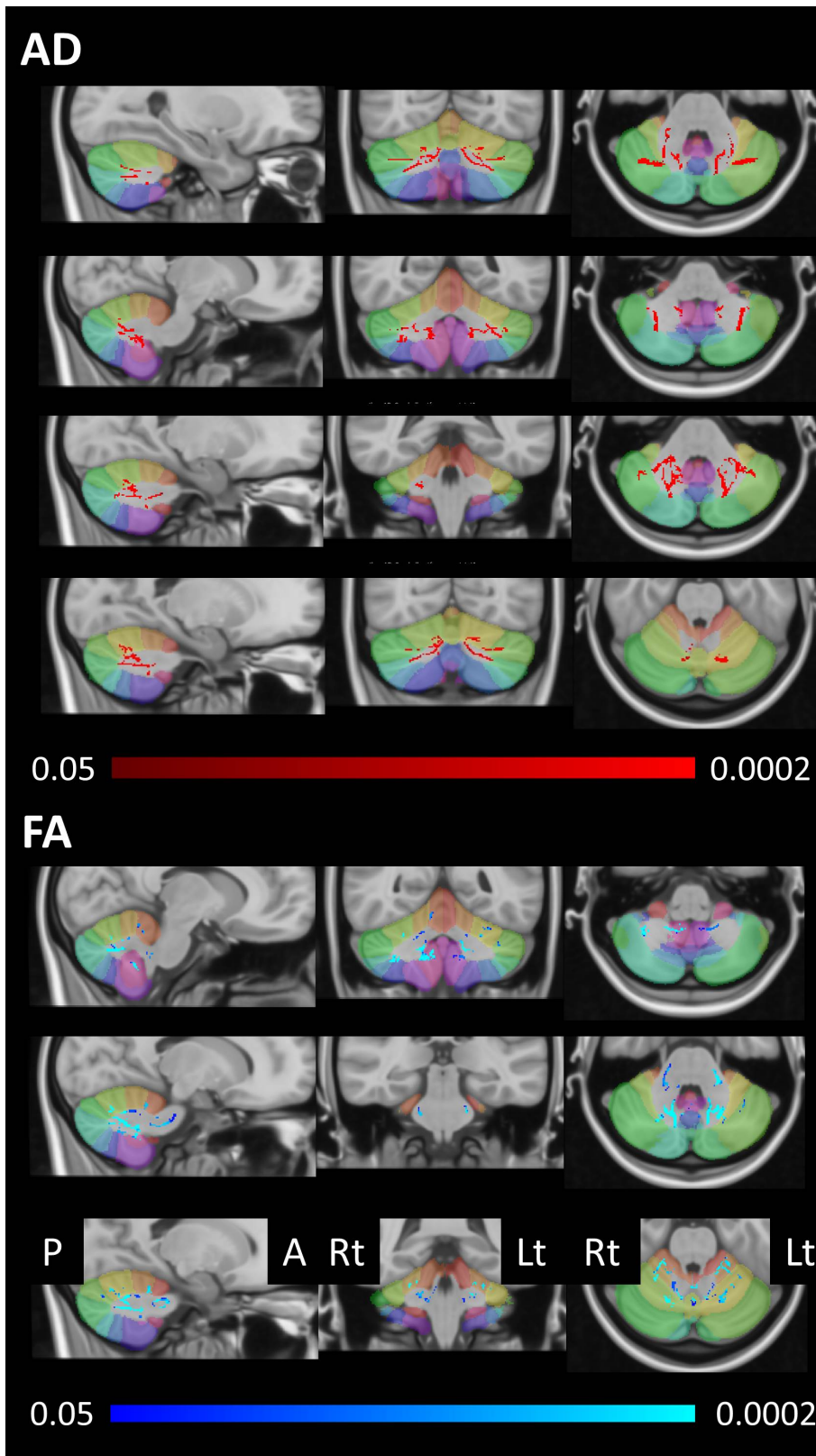


**Fig. 2.** Voxelwise patterns of increased fractional anisotropy (FA) and reduced axial diffusivity (AD) in poliomyelitis survivors as identified by tract-based spatial statistics at  $p < 0.05$  TFCE adjusted for age and gender. The labels of the Diedrichsen probabilistic cerebellar atlas are shown as underlay to aid localisation. Radiological convention is used, first column presents sagittal views, second column shows coronal views and last column depicts axial views. Lt, Left; Rt, Right; A, Anterior; P, Posterior.



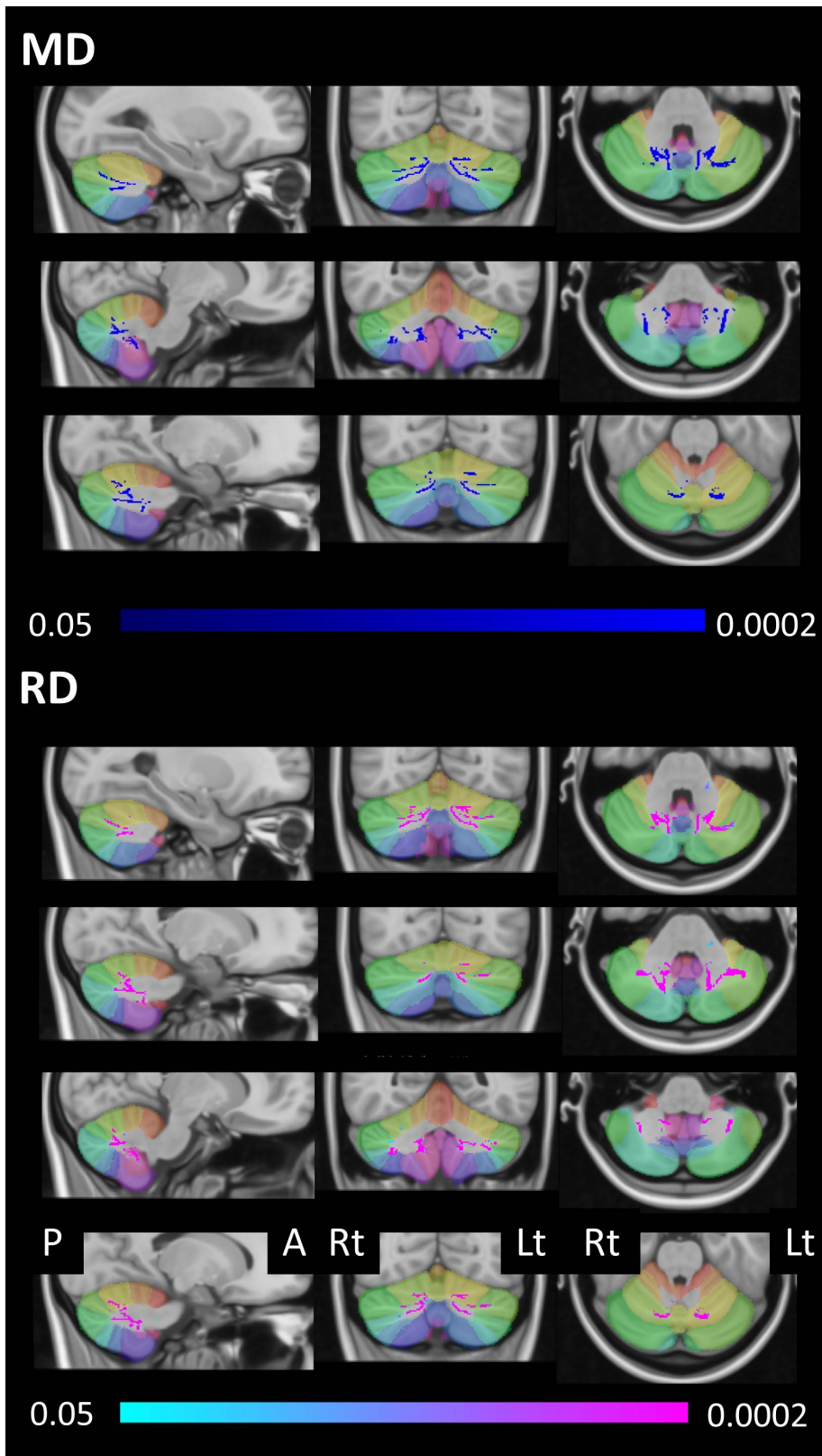


**Fig. 3.** Voxelwise patterns of reduced mean diffusivity (MD) and reduced radial diffusivity (RD) in poliomyelitis survivors as identified by tract-based spatial statistics at  $p < 0.05$  TFCE adjusted for age and gender. The labels of the Diedrichsen probabilistic cerebellar atlas are shown as underlay to aid localisation. Radiological convention is used, first column presents sagittal views, second column shows coronal views and last column depicts axial views. Lt, Left; Rt, Right; A, Anterior; P, Posterior.

**Table 2. Cerebellar cortical thickness in poliomyelitis survivors and healthy controls.**

Cerebellar region	Study group	EMM	Standard error	ANCOVA Sig. ( <i>p</i> )
Lobules I–II (right)	HC	1.345115	0.031503	0.038*
	Polio	1.465976	0.048126	
Lobules I–II (left)	HC	1.396892	0.034921	0.067 <sup>t</sup>
	Polio	1.514657	0.053347	
Lobule III (right)	HC	3.065033	0.031523	0.010*
	Polio	3.215933	0.048156	
Lobule III (left)	HC	3.187530	0.034797	0.065 <sup>t</sup>
	Polio	3.305935	0.053157	
Lobule IV (right)	HC	4.755922	0.017989	0.126
	Polio	4.806548	0.027480	
Lobule IV (left)	HC	4.904537	0.014732	0.709
	Polio	4.894459	0.022506	
Lobule V (right)	HC	4.737028	0.018026	0.915
	Polio	4.733494	0.027538	
Lobule V (left)	HC	4.898671	0.015243	0.891
	Polio	4.894833	0.023287	
Lobule VI (right)	HC	4.924036	0.011482	0.389
	Polio	4.905869	0.017540	
Lobule VI (left)	HC	4.974966	0.011298	0.319
	Polio	4.954307	0.017259	
Crus I (right)	HC	4.640872	0.024112	0.307
	Polio	4.595695	0.036835	
Crus I (left)	HC	4.581111	0.021624	0.076 <sup>t</sup>
	Polio	4.510507	0.033034	
Crus II (right)	HC	4.571318	0.025911	0.077 <sup>t</sup>
	Polio	4.486973	0.039582	
Crus II (left)	HC	4.375609	0.026474	0.853
	Polio	4.366600	0.040442	
Lobule VIIIB (right)	HC	4.786736	0.017746	0.143
	Polio	4.738892	0.027109	
Lobule VIIIB (left)	HC	4.612632	0.021329	0.518
	Polio	4.637905	0.032584	
Lobule VIIIA (right)	HC	4.635282	0.016534	0.046*
	Polio	4.696278	0.025258	
Lobule VIIIA (left)	HC	4.654906	0.017625	0.003*
	Polio	4.753642	0.026924	
Lobule VIIIB (right)	HC	4.557164	0.026441	0.001*
	Polio	4.726895	0.040393	
Lobule VIIIB (left)	HC	4.513289	0.03345	0.003*
	Polio	4.696155	0.051100	
Lobule IX (right)	HC	3.771612	0.039352	0.225
	Polio	3.859370	0.060116	
Lobule IX (left)	HC	3.588834	0.043782	0.866
	Polio	3.575345	0.066883	
Lobule X (right)	HC	2.244308	0.040101	0.938
	Polio	2.238572	0.061261	
Lobule X (left)	HC	2.479459	0.046601	0.402
	Polio	2.551171	0.071189	

Statistical comparisons are corrected for age and gender. Significant differences are flagged with \*, statistical trends with <sup>t</sup>. Polio, poliomyelitis survivors; HC, healthy controls; EMM, Estimated marginal means; ANCOVA, analysis of covariance.

right and left cerebellar hemispheres. As a quality control step, the accuracy of tissue-type segmentation and anatomical parcellation were individually reviewed for each subject. Cortical volume and thickness values were retrieved from lobules I–II, III, IV, V, VI, VIIIB, VIIIA, VIIIB, IX, X, Crus I and Crus II.

**Table 3. Cerebellar cortical volumes in poliomyelitis survivors and healthy controls.**

Cerebellar region	Study group	EMM	Standard error	ANCOVA Sig. ( <i>p</i> )
Lobules I–II (right)	HC	0.034213	0.001009	0.474
	Polio	0.035546	0.001547	
Lobules I–II (left)	HC	0.029124	0.001016	0.457
	Polio	0.027728	0.001558	
Lobule III (right)	HC	0.488477	0.009796	0.612
	Polio	0.497645	0.015020	
Lobule III (left)	HC	0.499655	0.010724	0.912
	Polio	0.497474	0.016443	
Lobule IV (right)	HC	1.928698	0.031254	0.550
	Polio	1.963218	0.047923	
Lobule IV (left)	HC	2.078443	0.032415	0.416
	Polio	2.029758	0.049704	
Lobule V (right)	HC	3.279021	0.045692	0.852
	Polio	3.263248	0.070061	
Lobule V (left)	HC	3.564292	0.044253	0.518
	Polio	3.511443	0.067855	
Lobule VI (right)	HC	7.870917	0.107912	0.890
	Polio	7.843433	0.156257	
Lobule VI (left)	HC	7.861064	0.106252	0.531
	Polio	7.983838	0.162921	
Crus I (right)	HC	11.118685	0.159449	0.531
	Polio	10.934478	0.244491	
Crus I (left)	HC	11.127808	0.165490	0.609
	Polio	10.971721	0.253753	
Crus II (right)	HC	7.018721	0.105569	0.344
	Polio	6.834148	0.161873	
Crus II (left)	HC	6.842425	0.099249	0.628
	Polio	6.753806	0.152183	
Lobule VIIIB (right)	HC	4.179157	0.058421	0.132
	Polio	4.016144	0.089580	
Lobule VIIIB (left)	HC	3.983546	0.060471	0.793
	Polio	3.954225	0.092722	
Lobule VIIIA (right)	HC	4.792981	0.066827	0.743
	Polio	4.752624	0.102469	
Lobule VIIIA (left)	HC	4.921682	0.068260	0.581
	Polio	4.991243	0.104667	
Lobule VIIIB (right)	HC	3.409387	0.059077	0.088
	Polio	3.596341	0.090585	
Lobule VIIIB (left)	HC	3.330394	0.051710	0.016*
	Polio	3.563492	0.079289	
Lobule IX (right)	HC	2.858097	0.042857	0.688
	Polio	2.889833	0.065714	
Lobule IX (left)	HC	2.698948	0.041592	0.818
	Polio	2.681282	0.063775	
Lobule X (right)	HC	0.574727	0.007499	0.519
	Polio	0.583663	0.011498	
Lobule X (left)	HC	0.575363	0.007213	0.060 <sup>t</sup>
	Polio	0.600540	0.011060	

Statistical comparisons are corrected for age, sex and intracranial volumes. Significant differences are flagged with \*, statistical trends with <sup>t</sup>. Polio, poliomyelitis survivors; HC, healthy controls; EMM, Estimated marginal means; ANCOVA, analysis of covariance.

## 2.5 Morphometry

Voxelwise grey matter changes were explored using region-of-interest morphometry in FMRIB's FSL suite. First, total intracranial volumes (TIV) were calculated for each participant, which was subsequently used as a covari-

**Table 4. Diffusivity alterations in cerebellar peduncles correcting for age and sex.**

Region	Study group	EMM	Standard error	ANCOVA Sig. ( <i>p</i> )
Fractional Anisotropy (FA)				
Superior peduncle (left)	HC	0.625407	0.004077	0.651
	Polio	0.621869	0.006394	
Superior peduncle (right)	HC	0.619614	0.004211	0.316
	Polio	0.611502	0.006603	
Middle peduncle	HC	0.520931	0.003512	0.001*
	Polio	0.543068	0.005507	
Inferior peduncle (left)	HC	0.516051	0.004326	0.045*
	Polio	0.499289	0.006784	
Inferior peduncle (right)	HC	0.512402	0.004462	0.061
	Polio	0.496299	0.006997	
Axial Diffusivity (AD)				
Superior peduncle (left)	HC	0.001380	0.000009	<0.001*
	Polio	0.001453	0.000014	
Superior peduncle (right)	HC	0.001398	0.000009	<0.001*
	Polio	0.001465	0.000014	
Middle peduncle	HC	0.001046	0.000005	0.774
	Polio	0.001043	0.000008	
Inferior peduncle (left)	HC	0.001081	0.000007	0.002*
	Polio	0.001122	0.000011	
Inferior peduncle (right)	HC	0.001092	0.000007	0.097
	Polio	0.001114	0.000011	
Radial Diffusivity (RD)				
Superior peduncle (left)	HC	0.000447	0.000006	0.016*
	Polio	0.000474	0.000009	
Superior peduncle (right)	HC	0.000464	0.000006	0.015*
	Polio	0.000492	0.000009	
Middle peduncle	HC	0.000433	0.000004	0.002*
	Polio	0.000410	0.000006	
Inferior peduncle (left)	HC	0.000460	0.000005	<0.001*
	Polio	0.000501	0.000007	
Inferior peduncle (right)	HC	0.000464	0.000005	0.001*
	Polio	0.000495	0.000007	
Mean Diffusivity (MD)				
Superior peduncle (left)	HC	0.000758	0.000006	<0.001*
	Polio	0.000800	0.000009	
Superior peduncle (right)	HC	0.000775	0.000006	<0.001*
	Polio	0.000817	0.000009	
Middle peduncle	HC	0.000638	0.000004	0.031*
	Polio	0.000621	0.000006	
Inferior peduncle (left)	HC	0.000667	0.000005	<0.001*
	Polio	0.000708	0.000007	
Inferior peduncle (right)	HC	0.000673	0.000005	0.002*
	Polio	0.000701	0.000007	

Significant differences are flagged with asterisk \*. Polio, poliomyelitis survivors; HC, healthy controls; EMM, Estimated marginal means; ANCOVA, analysis of covariance.

ate in the morphometric analyses and for the interpretation of lobular volumes. TIV calculations have been previously described [36,37], briefly, each participant's brain image was aligned to the MNI152 standard, and the inverse of the determinant of the affine registration matrix was calculated and multiplied by the size of the template. For spatial registration, FMRIB's FSL-FLIRT and for tissue type segmentation, FSL-FAST was utilised. Output partial grey matter, white matter and CSF volumes were added to determine TIV. Raw T1w data underwent skull-

removal (BET), motion-corrections and tissue-type segmentation. The accuracy of skull removal and segmentation was visually inspected in each subject for quality control. Individual grey-matter partial volume images were aligned to the MNI152 standard space using affine registration. Permutation-based non-parametric inference was for the voxelwise analyses implementing the threshold-free cluster enhancement (TFCE) method. Design matrices included group membership, age, sex and TIV. Voxelwise statistics were run in the cerebellar mask derived from 'label 1' of the MNI structural atlas [38]. Output statistical maps were thresholded at  $p < 0.05$  FWE TFCE and the Diedrichsen probabilistic atlas was used as underlay to help the localisation of statistically significant clusters.

## 2.6 Voxelwise white matter analyses

Subsequent to eddy current corrections and skull removal; a tensor model was then fitted to the raw diffusion data in FSL to generate maps of axial diffusivity (AD), fractional anisotropy (FA), mean diffusivity (MD) and radial diffusivity (RD). For non-linear registration and skeletonisation of individual images, FMRIB's software library's tract-based statistics module was utilised. For the two-way, voxelwise comparison of diffusivity parameters between poliomyelitis survivors and healthy controls permutation-based non-parametric inference was used restricting the analyses the cerebellar portion of the study-specific white matter skeleton. The design matrix used for permutation included group-membership, and age and sex as covariates. The threshold-free cluster enhancement (TFCE) method was applied and results considered significant at a  $p < 0.01$  TFCE family-wise error (FWE).

## 2.7 Cerebellar peduncle assessments

The labels (1, 11, 12, 13, 14) of the JHU-ICBM atlas was utilised to generate masks for the left and right inferior cerebellar peduncles, the middle cerebellar peduncle, and the left and right superior cerebellar peduncles. Average FA, AD, MD and RD values were retrieved from the merged skeletonised diffusion data using these masks from each subject for subsequent group comparisons.

## 3. Results

The demographic profile of healthy controls and polio survivors are summarised in Table 1. While the healthy controls were age- and gender- matched, they were also included as covariates in our analyses.

### 3.1 Cortical thickness analyses

Compared to healthy controls, polio survivors exhibited increased cortical thickness in lobules I–II, and lobule III in the right hemisphere, and in lobules VIIIA and VIIIB bilaterally controlling for age and sex (Table 2). A trend in increased cortical thickness was also detected in lobules I–II and III in the left hemisphere. No frank cortical thinning

was identified, but a trend of cortical thinning was noted in the left Crus I and right Crus II in poliomyelitis survivors.

### 3.2 Grey matter volumes

Increased grey matter volume was detected in the left lobule VIIIB of poliomyelitis survivors. A trend for increased grey matter volume was also observed in lobule X of the left cerebellar hemisphere (Table 3).

### 3.3 Cerebellar peduncles analyses

Diffusivity alterations in the cerebellar peduncles are presented in Table 4.

Higher fractional anisotropy was detected in middle cerebellar peduncle and lower FA in the left inferior peduncle. In the superior cerebellar peduncles, higher AD, RD and MD were identified.

### 3.4 Voxel-wise analyses

No foci of cerebellar atrophy were identified in poliomyelitis survivors. Voxel-wise grey matter analyses revealed increased grey matter partial volumes in lobules VI–IIb and IX bilaterally, and in lobules VI, VIIa and crus I in the left cerebellar hemisphere in poliomyelitis survivors in contrast to healthy controls adjusting for age, sex and TIV (Fig. 1). On voxel-wise analyses of white matter microstructure, higher FA and lower AD, RD and MD were detected in lobules VI and IX and crus I bilaterally in adult poliomyelitis survivors with reference to healthy controls (Figs. 2,3). Polio survivors also exhibited higher FA in lobule V and lower AD, RD and MD in crus II bilaterally compared to healthy individuals. Lastly, compared to healthy controls, higher FA with lower AD was detected bilaterally in the middle cerebellar peduncles of adult polio survivors.

## 4. Discussion

Our study provides compelling *in vivo* evidence of cerebellar changes in adult poliomyelitis survivors with reference to healthy controls. In contrast to previous post-mortem studies [9,14,15] and sporadic clinical reports [16–18], the cohort of adult poliomyelitis survivors evaluated in this study did not exhibit cerebellar atrophy. On the contrary, polio survivors exhibited hypertrophic changes in the cerebellum. The changes were focal and relatively symmetrical, affecting selective cerebellar lobules as opposed to the entire cerebellum. Increased cortical thickness was detected in lobules I–III, VIIa and VIIb and increased grey matter volume was found in lobules VIIb. In addition to the higher cerebellar cortical thickness, our data also revealed increased white matter organisation in the cerebellar peduncles, in particular in the middle and inferior cerebellar peduncles. Anatomical patterns of increased grey matter metrics were relatively concordant across retrieved cortical thickness, cortical volume and morphometric analyses and the three analyses have unanimously demonstrated the lack of atrophic changes. The interpretation of increased grey matter thickness in an adult disease-cohort requires the

careful review of the literature as the vast majority of imaging studies report disease-associated patterns of atrophy instead of increased volumes [39–41]. It is conceivable that a reporting bias exists for neurodegenerative changes and also that one-way contrasts may sometimes be performed assuming that a given patient cohort exhibit atrophy with respect of demographically-matched healthy controls. Increased grey matter metrics, such as volumes, partial volumes, thickness etc. are often explored from an adaptive remodelling perspective, especially if the identified anatomical patterns of hypertrophy are congruent with function-specific cortical areas [42,43]. Adaptive cerebral reorganisation due to longstanding insult or slowly progressive neurodegenerative change is often described based on functional MRI observations, but rarely captured on structural imaging [43–46].

Given the striking disparity between the few post mortem studies in the 1940s describing degenerative changes soon after the acute infection, and our imaging study evaluating brain changes many decades after the infection, it is very conceivable that initial inflammatory changes gradually give way to cerebellar remodelling. This may reconcile the seemingly contradictory findings of post mortem descriptions following fulminant infection and our imaging findings many decades after the acute infection. Neuroplasticity refers to the unique ability for the nervous system to modify and reorganise itself both structurally and functionally in a dynamic manner in response to injury [47]. This process is well-recognised to be more efficient in children [48], especially during the first few years of life, when neurogenesis, synaptogenesis, synaptic pruning and myelin formation and remodelling is heightened [49]. This is supported by superior functional outcomes following CNS insult in young children compared to adults and has been demonstrated by functional recovery of language centres [50], visual systems [51,52] and sensorimotor networks [53,54]. Remarkable cerebellar recovery has been described in young patients with traumatic brain injury [55] and other forms of cerebellar degeneration [56]. Neuroplasticity is a particularly well-recognised trait of the cerebellum which plays a pivotal role in motor learning and adaptation of movement to environmental demands [57]. The term ‘cerebellar reserve’ has been coined for the structure’s unparalleled ability to recover from lesions and respond to supratentorial pathology [58]. In animal studies, motor training has led to glial hypertrophy, thickening of the molecular layer, synaptogenesis, and increased dendrite numbers in stellate cells [59–61]. Unique cerebellar plasticity has also been demonstrated in healthy populations such as musicians [62,63], athletes [64,65] and other performers [66] following motor training. Given the young age at which spinal cord insult occurred in our cohort, it is conceivable that cerebellar remodelling was particularly efficient during these critical years of motor control development.



The detected patterns of increased cerebellar metrics suggest function-specific foci. Lobules I–III of anterior lobe, and lobules VI, VIIa and VIIb of posterior lobe primarily mediate sensorimotor processes [23,67]. The somatotopic architecture of the cerebellum has been extensively investigated [24,68]. Paradigm-based functional neuroimaging studies suggest that lobules II–III represent the legs and toes with respect to both tactile stimulation and during motor tasks [69,70]. Injury of these lobules is thought to result in gait and posture ataxia or lower limb ataxia (lobules I–III, VIII and IX) [71,72]. These are the same lobules which exhibited hypertrophic alterations in our cohort of poliomyelitis survivors. Our voxelwise analyses also indicate increased lobule VI and lobule IX volumes. Lobule IX is considered essential for visually guided movement [73], while lobules VI has been implicated in motor learning [74]. Poliomyelitis survivors are predominantly affected in their lower extremities due to residual polio-induced musculoskeletal deformities such as leg-length discrepancy, asymmetrical muscle weakness and joint arthrodesis for which they have learned to compensate for with altered gait patterns, posture and balance [75] all of which are adaptive processes mediated by cerebellar motor learning.

Our diffusivity findings also indicate enhanced cerebellar peduncles integrity in poliomyelitis survivors decades after their infection, particularly in the middle (MCPs) and inferior cerebellar peduncles (ICPs). The superior cerebellar peduncles (SCPs) are the main cerebellar output projections from the deep cerebellar nuclei to the contralateral cerebral cortex via the thalamus, known as cerebello-thalamo-cortical (CTC) projections. The MCPs constitute entirely of afferent fibres from the contralateral cerebral cortex via the pontine nuclei, known as the cortico-ponto-cerebellar (CPC) tract. These two tracts form a closed feed-forward and feed-back loop that enables the cerebellum to modulate both motor and non-motor processes [76,77]. Anatomically, the ICP consists of both cerebellar efferent and afferent fibres integrating information from the vestibular nuclei, mediating eye movements and head positioning. The ICP also encompasses afferent spinal fibres carrying proprioceptive and cutaneous information from the limbs to the cerebellum, which are crucial for posture, locomotion and muscle control [78]. Higher FA and lower RD in middle cerebellar peduncles may be interpreted as fibre reorganisation and suggests well myelinated cortico-ponto-cerebellar tracts. MCP alterations have been described in musicians [79] and are thought to represent adaptive change to repetitive sensorimotor and cognitive demands. The progressive recruitment of the cerebellum to carry out motor tasks has been observed in several neurodegenerative conditions such as amyotrophic lateral sclerosis (ALS) [34,42,44], Parkinson's disease (PD) [80] and Huntington's disease (HD) [81]. However, it is more commonly detected as increased activation or increased metabolism on

functional imaging, and only rarely appreciated on structural imaging [82].

In motor neuron disorders there is a disproportionate emphasis on wet biomarkers [83,84], and existing imaging studies primarily focus on the description of atrophy patterns [85] and connectivity changes [86,87] underpinning specific clinical phenotypes [88,89]. The targeted characterisation of compensatory changes is seldom specifically pursued and adaptive structural alterations in particular are rarely evaluated [90]. Our observations may have implications for other cohorts with acute anterior horn injury, such as patients with spinal cord infarction or spinal cord injuries [91]. Depending on the anatomical extent and age at the primary insult, adaptive process may take place to improve functional outcomes, which provides a very strong rationale for meticulous multidisciplinary interventions such as individualised physiotherapy and occupation therapy. Our findings may also be of relevance for non-traumatic, non-vascular, lower motor neuron conditions, such as progressive muscular atrophy (PMA), spinal muscular atrophy (SMA), spinal-bulbar muscular atrophy (SBMA) or patients with LMN-predominant ALS [92–95]. Depending on the rate of progression of the underlying neurodegenerative process, attempted compensatory processes may be at play to mitigate or slow down functional decline. This further highlights that rehabilitation efforts are also very important in progressive neurodegenerative diseases, and not just in acute neurovascular conditions and following CNS trauma [96]. The presence of compensatory mechanisms may also explain the apparent divergence between disease burden and the functional profile in some MND phenotypes [97]. Compensatory processes may also delay symptom manifestation despite considerable presymptomatic pathology [98–100]. Beyond the academic interest of describing adaptive processes, the demonstration of marked cerebellar neuroplasticity highlights the pivotal role of multidisciplinary interventions, individualised physiotherapy, and exercise-based strategies such as postural control [56], sitting balance and walking exercises [101]. Our findings may also support the rationale for non-invasive plasticity-inducing electrostimulation as part of multidisciplinary rehabilitation strategies [102,103].

The juxtaposition of several imaging analyses permits a nuanced characterisation of grey and white matter remodelling. Multiple cerebellar lobules exhibited increased cortical thickness in poliomyelitis survivors, while increased grey matter volume was only detected in lobules VIIIB and X. This mirrors supratentorial observations in other conditions where cortical thickness measurements are often more sensitive to structural alterations than volume variables. Another benefit of appraising cortical thickness measures is that they don't require adjustments for TIV. The differing detection sensitivity of imaging indices highlight the importance of evaluating multiple parameters (thickness, volumes, voxelwise partial-volumes) to comprehensively eval-

uate grey matter changes. Similarly, the evaluation of multiple diffusivity indices provides indirect insights into the cellular underpinnings of white matter alterations. Diffusivity metrics are derived from main eigenvalues ( $\lambda_1$ ,  $\lambda_2$ ,  $\lambda_3$ ) and reflect on restriction characteristics of water movement along the length of the axon and perpendicular to the axon. FA and MD ( $(\lambda_1 + \lambda_2 + \lambda_3)/3$ ) are generic, composite markers of white matter microstructural integrity. Axial diffusivity ( $\lambda_1$ ) is commonly regarded as a marker of axonal integrity while radial diffusivity  $((\lambda_2 + \lambda_3)/2)$  is often seen as a proxy of myelin integrity [104,105]. While these associations are likely to be simplistic, in the absence of robust post mortem studies in poliomyelitis survivors, the assessment of multiple diffusivity metrics is particularly valuable.

This study is not without limitations. Our study has a cross-sectional design and included a relatively small sample of poliomyelitis survivors which precluded further stratification for age at initial infection or disability severity. We have only evaluated cerebral changes in this study, even though quantitative spinal protocols are increasingly available [106,107] and combined cord-brain studies are likely to elucidate proposed compensatory processes further. We also acknowledge the inherent inclusion bias to patients with less severe disability; the presented cohort of poliomyelitis survivors had minimal respiratory compromise and did not have severe scoliosis. Patients with severe polio-induced deformities were less likely to attend our research facility or tolerate the duration of the MRI protocol. Furthermore, our observations are mere snapshots of cerebellar architecture many decades after the original illness. The longitudinal trajectory of putative compensatory processes could not be explicitly demonstrated due to the cross-sectional design of the study. Notwithstanding these limitations, our findings suggest radiological evidence of cerebellar reorganisation decades after severe lower motor neuron injury. We hypothesise that similar compensatory process may occur in other spinal conditions and that the younger the age at initial injury, the more successful these processes may be. While these hypotheses remain to be confirmed in purpose-designed longitudinal protocols, our findings highlight the importance of specifically evaluating hypertrophic changes in neuroimaging studies instead of solely characterising patterns of atrophy.

## 5. Conclusions

The widespread cerebral changes described in the post mortem literature of poliomyelitis represent the acute sequelae of the infection. Pathological changes in the chronic phase, long after the infection, are poorly characterised. Our neuroimaging findings indicate considerable cerebellar reorganisation decades after poliomyelitis infection which may be interpreted as compensation to anterior horn insult in infancy. Similar processes may take place in other spinal cord conditions and in particular, in motor neuron disorders. Instead of exclusively focusing on neurodegenerative

changes, academic neuroimaging studies should also evaluate evidence for neuroplasticity and compensatory processes.

## Abbreviations

ALS, amyotrophic lateral sclerosis; ALSFRS-r, revised amyotrophic lateral sclerosis functional rating scale ANCOVA, analysis of covariance; ANOVA, analysis of variance; CPC, cortico-ponto-cerebellar tract; CTC, cerebello-thalamo-cortical tract; DTI, Diffusion Tensor Imaging; EMM, estimated marginal mean; FLAIR, Fluid-attenuated inversion recovery; FOV, field of view; FWE, familywise error; GM, grey matter; HC, healthy control; HSP, hereditary spastic paraplegia; ICP, inferior cerebellar peduncle; IR-SPGR, inversion recovery prepared spoiled gradient recalled echo; IR-TSE, inversion recovery turbo spin echo sequence; Lt, left; LL, Lower limb; LEoP, late effects of polio; LMN, lower motor neuron; MCP, middle cerebellar peduncle; MND, motor neuron disease; MNI152, Montreal Neurological Institute 152 standard space; PLS, primary lateral sclerosis; PPS, Post-polio syndrome; Rt, right; ROI, region of interest; SBMA, Spinal-bulbar muscular atrophy; SCP, superior cerebellar peduncle; SE-EPI, spin-echo echo planar imaging; SENSE, Sensitivity Encoding; SMA, Spinal muscular atrophy; SPIR, spectral presaturation with inversion recovery; T1w, T1-weighted imaging; TE, Echo time; TFCE, threshold-free cluster enhancement; TI, Inversion time; TIV, total intracranial volume; TR, repetition time; UL, Upper limb; UMN, Upper motor neuron.

## Author contributions

Drafting the manuscript—SLHS, PB. Neuroimaging analyses—SLHS, AM, JL, PB. Conceptualisation of the study—SLHS, PB. Revision of the manuscript for intellectual content—SLHS, AM, JL, OH, PB.

## Ethics approval and consent to participate

This study was approved by the Ethics (Medical Research) Committee (08/90)—Beaumont Hospital, Dublin, Ireland.

## Acknowledgment

We express our gratitude to all patients and healthy controls for participating in this research study. Without their contribution, this study would not have been possible.

## Funding

Professor Bede and the computational neuroimaging group are supported by the Health Research Board (HRB EIA-2017-019 and HRB JPND-CoFund-2019), the Spastic Paraplegia Foundation (SPF), the EU Joint Programme – Neurodegenerative Disease Research (JPND), the Andrew Lydon scholarship, the Irish Institute of Clinical Neuroscience (IICN), and the Iris O'Brien Foundation.

## Conflict of interest

The authors declare no conflict of interest.

## References

- [1] World Health Organization. Poliomyelitis. 2019. Available at: <https://www.who.int/news-room/fact-sheets/detail/poliomyelitis> (Accessed: 19 October 2021).
- [2] Mehndiratta MM, Mehndiratta P, Pande R. Poliomyelitis: historical facts, epidemiology, and current challenges in eradication. *The Neurohospitalist*. 2014; 4: 223–229.
- [3] Gonzalez H, Olsson T, Borg K. Management of postpolio syndrome. *The Lancet Neurology*. 2010; 9: 634–642.
- [4] March of Dimes. Post-polio syndrome: identifying best practices in diagnosis & care. 2001. Available at: <https://www.polioplace.org/sites/default/files/files/MOD-%20Identifying.pdf> (Accessed: 19 October 2021).
- [5] Ramlow J, Alexander M, LaPorte R, Kaufmann C, Kuller L. Epidemiology of the post-polio syndrome. *American Journal of Epidemiology*. 1992; 136: 769–786.
- [6] Cosgrove JL, Alexander MA, Kitts EL, Swan BE, Klein MJ, Bauer RE. Late effects of poliomyelitis. *Archives of Physical Medicine and Rehabilitation*. 1987; 68: 4–7.
- [7] Li Hi Shing S, Chipika RH, Finegan E, Murray D, Hardiman O, Bede P. Post-polio Syndrome: more than Just a Lower Motor Neuron Disease. *Frontiers in Neurology*. 2019; 10: 773.
- [8] Luhan JA. Epidemic poliomyelitis; some pathologic observations on human material. *Archives of Pathology*. 1946; 42: 245–260.
- [9] Bodian D. Histopathologic basis of clinical findings in poliomyelitis. *The American Journal of Medicine*. 1949; 6: 563–578.
- [10] Bodian D. Poliomyelitis; neuropathologic observations in relation to motor symptoms. *Journal of the American Medical Association*. 1947; 134: 1148–1154.
- [11] Barnhart M, Rhines R. Distribution of lesions of the brain stem in poliomyelitis. *Archives of Neurology and Psychiatry*. 1948; 59: 368–377.
- [12] Jubelt B, Gallez-Hawkins G, Narayan O, Johnson RT. Pathogenesis of human poliovirus infection in mice. i. Clinical and pathological studies. *Journal of Neuropathology and Experimental Neurology*. 1980; 39: 138–148.
- [13] Ford DJ, Ropka SL, Collins GH, Jubelt B. The neuropathology observed in wild-type mice inoculated with human poliovirus mirrors human paralytic poliomyelitis. *Microbial Pathogenesis*. 2002; 33: 97–107.
- [14] Swan C. The anatomical distribution and character of the lesions of poliomyelitis. *Australian Journal of Experimental Biology and Medical Science*. 1939; 17: 345–364.
- [15] Baker AB. Poliomyelitis. a.M.a. *Archives of Neurology & Psychiatry*. 1954; 71: 455.
- [16] Curnen EC, Chamberlin HR. Acute cerebellar ataxia associated with poliovirus infection. *The Yale Journal of Biology and Medicine*. 1961; 34: 219–233.
- [17] Berglund G, Mossberg HO, Rydenstam B. Acute cerebellar ataxia in children. *Acta Paediatrica*. 1955; 44: 254–262.
- [18] Meindez Cashion D, Sanchez-longo LP, Valcarcel M, Rosen L. Acute cerebellar ataxia in children associated with infection by poliovirus i. *Pediatrics*. 1962; 29: 808–815.
- [19] Oliveri M, Brighina F, La Bua V, Buffa D, Aloisio A, Fierro B. Reorganization of cortical motor area in prior polio patients. *Clinical Neurophysiology*. 1999; 110: 806–812.
- [20] Lupu VD, Danielian L, Johnsen JA, Vasconcelos OM, Prokhorenko OA, Jabbari B, *et al.* Physiology of the motor cortex in polio survivors. *Muscle & Nerve*. 2008; 37: 177–182.
- [21] Li Hi Shing S, Lope J, McKenna MC, Chipika RH, Hardiman O, Bede P. Increased cerebral integrity metrics in poliomyelitis survivors: putative adaptation to longstanding lower motor neuron degeneration. *Journal of the Neurological Sciences*. 2021; 424: 117361.
- [22] Koziol LF, Budding D, Andreasen N, D'Arrigo S, Bulgheroni S, Imamizu H, *et al.* Consensus paper: the cerebellum's role in movement and cognition. *Cerebellum*. 2014; 13: 151–177.
- [23] Stoodley CJ, Schmahmann JD. Evidence for topographic organization in the cerebellum of motor control versus cognitive and affective processing. *Cortex*. 2010; 46: 831–844.
- [24] Buckner RL, Krienen FM, Castellanos A, Diaz JC, Yeo BTT. The organization of the human cerebellum estimated by intrinsic functional connectivity. *Journal of Neurophysiology*. 2011; 106: 2322–2345.
- [25] Chipika RH, Finegan E, Li Hi Shing S, McKenna MC, Christidi F, Chang KM, *et al.* "Switchboard" malfunction in motor neuron diseases: Selective pathology of thalamic nuclei in amyotrophic lateral sclerosis and primary lateral sclerosis. *NeuroImage: Clinical*. 2020; 27: 102300.
- [26] Chipika RH, Christidi F, Finegan E, Li Hi Shing S, McKenna MC, Chang KM, *et al.* Amygdala pathology in amyotrophic lateral sclerosis and primary lateral sclerosis. *Journal of the Neurological Sciences*. 2020; 417: 117039.
- [27] Finegan E, Chipika RH, Shing SLH, Hardiman O, Bede P. Primary lateral sclerosis: a distinct entity or part of the ALS spectrum? *Amyotrophic Lateral Sclerosis and Frontotemporal Degeneration*. 2019; 20: 133–145.
- [28] Finegan E, Shing SLH, Chipika RH, Chang KM, McKenna MC, Doherty MA, *et al.* Extra-motor cerebral changes and manifestations in primary lateral sclerosis. *Brain Imaging and Behavior*. 2021; 15: 2283–2296.
- [29] Burke T, Pinto-Grau M, Lonergan K, Elamin M, Bede P, Costello E, *et al.* Measurement of Social Cognition in Amyotrophic Lateral Sclerosis: a Population Based Study. *PLoS ONE*. 2016; 11: e0160850.
- [30] Burke T, Elamin M, Bede P, Pinto-Grau M, Lonergan K, Hardiman O, *et al.* Discordant performance on the 'Reading the Mind in the Eyes' Test, based on disease onset in amyotrophic lateral sclerosis. *Amyotrophic Lateral Sclerosis & Frontotemporal Degeneration*. 2016; 17: 467–472.
- [31] Yunusova Y, Plowman EK, Green JR, Barnett C, Bede P. Clinical Measures of Bulbar Dysfunction in ALS. *Frontiers in Neurology*. 2019; 10: 106.
- [32] Finegan E, Chipika RH, Li Hi Shing S, Hardiman O, Bede P. Pathological Crying and Laughing in Motor Neuron Disease: Pathobiology, Screening, Intervention. *Frontiers in Neurology*. 2019; 10: 260.
- [33] Bede P, Finegan E. Revisiting the pathoanatomy of pseudobulbar affect: mechanisms beyond corticobulbar dysfunction. *Amyotrophic Lateral Sclerosis & Frontotemporal Degeneration*. 2018; 19: 4–6.
- [34] Prell T, Grosskreutz J. The involvement of the cerebellum in amyotrophic lateral sclerosis. *Amyotrophic Lateral Sclerosis & Frontotemporal Degeneration*. 2013; 14: 507–515.
- [35] Cedarbaum JM, Stambler N, Malta E, Fuller C, Hilt D, Thurmond B, *et al.* The ALSFRS-R: a revised ALS functional rating scale that incorporates assessments of respiratory function. BDNF ALS Study Group (Phase III). *Journal of the Neurological Sciences*. 1999; 169: 13–21.
- [36] Bede P, Chipika RH, Finegan E, Li Hi Shing S, Doherty MA, Hengeveld JC, *et al.* Brainstem pathology in amyotrophic lateral sclerosis and primary lateral sclerosis: a longitudinal neuroimaging study. *NeuroImage: Clinical*. 2019; 24: 102054.
- [37] Christidi F, Karavasilis E, Rentzos M, Velonakis G, Zouvelou V, Xirou S, *et al.* Hippocampal pathology in amyotrophic lateral sclerosis: selective vulnerability of subfields and their associated projections. *Neurobiology of Aging*. 2019; 84: 178–188.



- [38] Bede P, Chipika RH, Christidi F, Hengeveld JC, Karavasilis E, Argyropoulos GD, *et al.* Genotype-associated cerebellar profiles in ALS: focal cerebellar pathology and cerebro-cerebellar connectivity alterations. *Journal of Neurology, Neurosurgery & Psychiatry*. 2021; 92: 1197–1205.
- [39] Finegan E, Chipika RH, Li Hi Shing S, Doherty MA, Hengeveld JC, Vajda A, *et al.* The clinical and radiological profile of primary lateral sclerosis: a population-based study. *Journal of Neurology*. 2019; 266: 2718–2733.
- [40] Dukic S, McMackin R, Buxo T, Fasano A, Chipika R, Pinto-Grau M, *et al.* Patterned functional network disruption in amyotrophic lateral sclerosis. *Human Brain Mapping*. 2019; 40: 4827–4842.
- [41] Finegan E, Li Hi Shing S, Chipika RH, Doherty MA, Hengeveld JC, Vajda A, *et al.* Widespread subcortical grey matter degeneration in primary lateral sclerosis: a multimodal imaging study with genetic profiling. *NeuroImage: Clinical*. 2019; 24: 102089.
- [42] Abidi M, Marco G, Couillandre A, Feron M, Mseddi E, Termoz N, *et al.* Adaptive functional reorganization in amyotrophic lateral sclerosis: coexisting degenerative and compensatory changes. *European Journal of Neurology*. 2020; 27: 121–128.
- [43] Querin G, El Mendili M, Lenglet T, Behin A, Stojkovic T, Salachas F, *et al.* The spinal and cerebral profile of adult spinal-muscular atrophy: a multimodal imaging study. *NeuroImage: Clinical*. 2019; 21: 101618.
- [44] Abidi M, Marco G, Grami F, Termoz N, Couillandre A, Querin G, *et al.* Neural Correlates of Motor Imagery of Gait in Amyotrophic Lateral Sclerosis. *Journal of Magnetic Resonance Imaging*. 2021; 53: 223–233.
- [45] Feron M, Couillandre A, Mseddi E, Termoz N, Abidi M, Bardin E, *et al.* Extrapyramidal deficits in ALS: a combined biomechanical and neuroimaging study. *Journal of Neurology*. 2018; 265: 2125–2136.
- [46] Proudfoot M, Bede P, Turner MR. Imaging Cerebral Activity in Amyotrophic Lateral Sclerosis. *Frontiers in Neurology*. 2018; 9: 1148.
- [47] Cramer SC, Sur M, Dobkin BH, O'Brien C, Sanger TD, Trojanowski JQ, *et al.* Harnessing neuroplasticity for clinical applications. *Brain*. 2011; 134: 1591–1609.
- [48] Kleim JA, Jones TA. Principles of experience-dependent neural plasticity: implications for rehabilitation after brain damage. *Journal of Speech, Language, and Hearing Research*. 2008; 51: S225–S239.
- [49] Ismail FY, Fatemi A, Johnston MV. Cerebral plasticity: Windows of opportunity in the developing brain. *European Journal of Paediatric Neurology*. 2017; 21: 23–48.
- [50] Bates E, Reilly J, Wulfeck B, Dronkers N, Opie M, Fenson J, *et al.* Differential effects of unilateral lesions on language production in children and adults. *Brain and Language*. 2001; 79: 223–265.
- [51] Guzzetta A, D'Acunto G, Rose S, Tinelli F, Boyd R, Cioni G. Plasticity of the visual system after early brain damage. *Developmental Medicine and Child Neurology*. 2010; 52: 891–900.
- [52] Werth R. Cerebral blindness and plasticity of the visual system in children. A review of visual capacities in patients with occipital lesions, hemispherectomy or hydranencephaly. *Restorative Neurology and Neuroscience*. 2008; 26: 377–389.
- [53] Artzi M, Shiran SI, Weinstein M, Myers V, Tarrasch R, Schertz M, *et al.* Cortical Reorganization following Injury Early in Life. *Neural Plasticity*. 2016; 2016: 1–9.
- [54] Szulc-Lerch KU, Timmons BW, Bouffet E, Laughlin S, de Medeiros CB, Skocic J, *et al.* Repairing the brain with physical exercise: Cortical thickness and brain volume increases in long-term pediatric brain tumor survivors in response to a structured exercise intervention. *NeuroImage: Clinical*. 2018; 18: 972–985.
- [55] Drijkoningen D, Caeyenberghs K, Leunissen I, Vander Linden C, Leemans A, Sunaert S, *et al.* Training-induced improvements in postural control are accompanied by alterations in cerebellar white matter in brain injured patients. *NeuroImage: Clinical*. 2015; 7: 240–251.
- [56] Burciu RG, Fritsche N, Granert O, Schmitz L, Spönnemann N, Konczak J, *et al.* Brain changes associated with postural training in patients with cerebellar degeneration: a voxel-based morphometry study. *The Journal of Neuroscience*. 2013; 33: 4594–4604.
- [57] Marino, Jr. R, Machado AGG, Timo-Iaria C. Functional Recovery after Combined Cerebral and Cerebellar Hemispherectomy in the Rat. *Stereotactic and Functional Neurosurgery*. 2001; 76: 83–93.
- [58] Mitoma H, Buffo A, Gelfo F, Guell X, Fucà E, Kakei S, *et al.* Consensus Paper. Cerebellar Reserve: from Cerebellar Physiology to Cerebellar Disorders. *The Cerebellum*. 2020; 19: 131–153.
- [59] Stevenson ME, Nazario AS, Czyn AM, Owen HA, Swain RA. Motor learning rapidly increases synaptogenesis and astrocytic structural plasticity in the rat cerebellum. *Neurobiology of Learning and Memory*. 2021; 177: 107339.
- [60] Anderson BJ, Li X, Alcantara AA, Isaacs KR, Black JE, Greenough WT. Glial hypertrophy is associated with synaptogenesis following motor-skill learning, but not with angiogenesis following exercise. *Glia*. 1994; 11: 73–80.
- [61] González-Tapia D, González-Ramírez MM, Vázquez-Hernández N, González-Burgos I. Motor learning induces plastic changes in Purkinje cell dendritic spines in the rat cerebellum. *Neurología*. 2020; 35: 451–457.
- [62] Bruchhage MMK, Amad A, Draper SB, Seidman J, Lacerda L, Laguna PL, *et al.* Drum training induces long-term plasticity in the cerebellum and connected cortical thickness. *Scientific Reports*. 2020; 10: 10116.
- [63] Hutchinson S, Lee LH, Gaab N, Schlaug G. Cerebellar volume of musicians. *Cerebral Cortex*. 2003; 13: 943–949.
- [64] Park IS, Lee KJ, Han JW, Lee NJ, Lee WT, Park KA, *et al.* Experience-dependent plasticity of cerebellar vermis in basketball players. *Cerebellum*. 2009; 8: 334–339.
- [65] Park IS, Lee YN, Kwon S, Lee NJ, Rhyu IJ. White matter plasticity in the cerebellum of elite basketball athletes. *Anatomy & Cell Biology*. 2015; 48: 262–267.
- [66] Hänggi J, Koenke S, Bezzola L, Jäncke L. Structural neuroplasticity in the sensorimotor network of professional female ballet dancers. *Human Brain Mapping*. 2010; 31: 1196–1206.
- [67] Stoodley CJ, Valera EM, Schmahmann JD. An fMRI study of intra-individual functional topography in the human cerebellum. *Behavioural Neurology*. 2010; 23: 65–79.
- [68] Boillat Y, Bazin P, van der Zwaag W. Whole-body somatotopic maps in the cerebellum revealed with 7T fMRI. *NeuroImage*. 2020; 211: 116624.
- [69] Nitschke MF, Kleinschmidt A, Wessel K, Frahm J. Somatotopic motor representation in the human anterior cerebellum. A high-resolution functional MRI study. *Brain*. 1996; 119: 1023–1029.
- [70] Grodd W, Hülsmann E, Lotze M, Wildgruber D, Erb M. Sensorimotor mapping of the human cerebellum: fMRI evidence of somatotopic organization. *Human Brain Mapping*. 2001; 13: 55–73.
- [71] Konczak J, Schoch B, Dimitrova A, Gizewski E, Timmann D. Functional recovery of children and adolescents after cerebellar tumour resection. *Brain*. 2005; 128: 1428–1441.
- [72] Schoch B, Konczak J, Dimitrova A, Gizewski ER, Wieland R, Timmann D. Impact of surgery and adjuvant therapy on balance function in children and adolescents with cerebellar tumors. *Neuropediatrics*. 2006; 37: 350–358.
- [73] Glickstein M, Gerrits N, Kralj-Hans I, Mercier B, Stein J, Voogd J. Visual pontocerebellar projections in the macaque. *The Journal of Comparative Neurology*. 1994; 349: 51–72.



- [74] Bernard JA, Seidler RD. Cerebellar contributions to visuomotor adaptation and motor sequence learning: an ALE meta-analysis. *Frontiers in Human Neuroscience*. 2013; 7: 27.
- [75] Ploeger HE, Bus SA, Nollet F, Brehm M. Gait patterns in association with underlying impairments in polio survivors with calf muscle weakness. *Gait & Posture*. 2017; 58: 146–153.
- [76] Palesi F, De Rinaldis A, Castellazzi G, Calamante F, Muhlert N, Chard D, *et al.* Contralateral cortico-ponto-cerebellar pathways reconstruction in humans *in vivo*: implications for reciprocal cerebro-cerebellar structural connectivity in motor and non-motor areas. *Scientific Reports*. 2017; 7: 12841.
- [77] Ramnani N. The primate cortico-cerebellar system: anatomy and function. *Nature Reviews. Neuroscience*. 2006; 7: 511–522.
- [78] Thach WT, Bastian AJ. Role of the cerebellum in the control and adaptation of gait in health and disease. *Progress in Brain Research*. 2004; 143: 353–366.
- [79] Abdul-Kareem IA, Stancak A, Parkes LM, Al-Ameen M, Alghamdi J, Aldhafeeri FM, *et al.* Plasticity of the superior and middle cerebellar peduncles in musicians revealed by quantitative analysis of volume and number of streamlines based on diffusion tensor tractography. *Cerebellum*. 2011; 10: 611–623.
- [80] Simioni AC, Dagher A, Fellows LK. Compensatory striatal-cerebellar connectivity in mild-moderate Parkinson's disease. *NeuroImage*. 2016; 10: 54–62.
- [81] Tereshchenko AV, Schultz JL, Bruss JE, Magnotta VA, Epping EA, Nopoulos PC. Abnormal development of cerebellar-striatal circuitry in Huntington disease. *Neurology*. 2020; 94: e1908–e1915.
- [82] Qiu T, Zhang Y, Tang X, Liu X, Wang Y, Zhou C, *et al.* Precentral degeneration and cerebellar compensation in amyotrophic lateral sclerosis: A multimodal MRI analysis. *Human Brain Mapping*. 2019; 40: 3464–3474.
- [83] Blasco H, Patin F, Descat A, Garçon G, Corcia P, Gelé P, *et al.* A pharmaco-metabolomics approach in a clinical trial of ALS: Identification of predictive markers of progression. *PLoS ONE*. 2018; 13: e0198116.
- [84] Devos D, Moreau C, Kyheng M, Garçon G, Rolland AS, Blasco H, *et al.* A ferroptosis-based panel of prognostic biomarkers for Amyotrophic Lateral Sclerosis. *Scientific Reports*. 2019; 9: 2918.
- [85] Bede P, Iyer PM, Schuster C, Elamin M, McLaughlin RL, Kenna K, *et al.* The selective anatomical vulnerability of ALS: 'disease-defining' and 'disease-defying' brain regions. *Amyotrophic Lateral Sclerosis & Frontotemporal Degeneration*. 2016; 17: 561–570.
- [86] Meier JM, Burgh HK, Nitert AD, Bede P, Lange SC, Hardiman O, *et al.* Connectome-Based Propagation Model in Amyotrophic Lateral Sclerosis. *Annals of Neurology*. 2020; 87: 725–738.
- [87] Nasserouleslami B, Dukic S, Broderick M, Mohr K, Schuster C, Gavin B, *et al.* Characteristic Increases in EEG Connectivity Correlate with Changes of Structural MRI in Amyotrophic Lateral Sclerosis. *Cerebral Cortex*. 2019; 29: 27–41.
- [88] Finegan E, Li Hi Shing S, Siah WF, Chipika RH, Chang KM, McKenna MC, *et al.* Evolving diagnostic criteria in primary lateral sclerosis: the clinical and radiological basis of "probable PLS". *Journal of the Neurological Sciences*. 2020; 417: 117052.
- [89] Bede P, Querin G, Pradat P. The changing landscape of motor neuron disease imaging: the transition from descriptive studies to precision clinical tools. *Current Opinion in Neurology*. 2018; 31: 431–438.
- [90] Bede P, Bogdahn U, Lope J, Chang K, Xirou S, Christidi F. Degenerative and regenerative processes in amyotrophic lateral sclerosis: motor reserve, adaptation and putative compensatory changes. *Neural Regeneration Research*. 2021; 16: 1208.
- [91] Leboutoux M, Franques J, Guillemin R, Delmont E, Lenglet T, Bede P, *et al.* Revisiting the spectrum of lower motor neuron diseases with snake eyes appearance on magnetic resonance imaging. *European Journal of Neurology*. 2014; 21: 1233–1241.
- [92] Pradat P, Bernard E, Corcia P, Couratier P, Jublanc C, Querin G, *et al.* The French national protocol for Kennedy's disease (SBMA): consensus diagnostic and management recommendations. *Orphanet Journal of Rare Diseases*. 2020; 15: 90.
- [93] Querin G, Bede P, Marchand-Pauvert V, Pradat P. Biomarkers of Spinal and Bulbar Muscle Atrophy (SBMA): a Comprehensive Review. *Frontiers in Neurology*. 2018; 9: 844.
- [94] Querin G, Lenglet T, Debs R, Stojkovic T, Behin A, Salachas F, *et al.* The motor unit number index (MUNIX) profile of patients with adult spinal muscular atrophy. *Clinical Neurophysiology*. 2018; 129: 2333–2340.
- [95] Querin G, Lenglet T, Debs R, Stojkovic T, Behin A, Salachas F, *et al.* Development of new outcome measures for adult SMA type III and IV: a multimodal longitudinal study. *Journal of Neurology*. 2021; 268: 1792–1802.
- [96] Hardiman O, Doherty CP, Elamin M, Bede P. *Neurodegenerative Disorders: A Clinical Guide* (pp. 1–336). Springer Cham Heidelberg New York Dordrecht London© Springer International Publishing Switzerland 2016: Springer International Publishing. 2016.
- [97] Verstraete E, Turner MR, Grosskreutz J, Filippi M, Benatar M. Mind the gap: the mismatch between clinical and imaging metrics in ALS. *Amyotrophic Lateral Sclerosis & Frontotemporal Degeneration*. 2015; 16: 524–529.
- [98] Lulé DE, Müller H, Finsel J, Weydt P, Knehr A, Winthor I, *et al.* Deficits in verbal fluency in presymptomatic C9orf72 mutation gene carriers—a developmental disorder. *Journal of Neurology, Neurosurgery & Psychiatry*. 2020; 91: 1195–1200.
- [99] Chipika RH, Siah WF, McKenna MC, Li Hi Shing S, Hardiman O, Bede P. The presymptomatic phase of amyotrophic lateral sclerosis: are we merely scratching the surface? *Journal of Neurology*. 2020. (in press)
- [100] Querin G, Bede P, El Mendili MM, Li M, Pélégri-Isaac M, Rinaldi D, *et al.* Presymptomatic spinal cord pathology in c9orf72 mutation carriers: A longitudinal neuroimaging study. *Annals of Neurology*. 2019; 86: 158–167.
- [101] Keller JL, Bastian AJ. A home balance exercise program improves walking in people with cerebellar ataxia. *Neurorehabilitation and Neural Repair*. 2014; 28: 770–778.
- [102] D'Mello AM, Turkeltaub PE, Stoodley CJ. Cerebellar tDCS Modulates Neural Circuits during Semantic Prediction: a Combined tDCS-fMRI Study. *The Journal of Neuroscience*. 2017; 37: 1604–1613.
- [103] Mitoma H, Manto M, Gandini J. Gandini. Recent Advances in the Treatment of Cerebellar Disorders. *Brain Sciences*. 2019; 10: 11.
- [104] Budde MD, Xie M, Cross AH, Song S-. Axial Diffusivity is the Primary Correlate of Axonal Injury in the Experimental Autoimmune Encephalomyelitis Spinal Cord: a Quantitative Pixelwise Analysis. *Journal of Neuroscience*. 2009; 29: 2805–2813.
- [105] Song S, Yoshino J, Le TQ, Lin S, Sun S, Cross AH, *et al.* Demyelination increases radial diffusivity in corpus callosum of mouse brain. *NeuroImage*. 2005; 26: 132–140.
- [106] El Mendili MM, Querin G, Bede P, Pradat PF. Pradat. Spinal Cord Imaging in Amyotrophic Lateral Sclerosis: Historical Concepts-Novel Techniques. *Frontiers in Neurology*. 2019; 10: 350.
- [107] Querin G, El Mendili MM, Bede P, Delphine S, Lenglet T, Marchand-Pauvert V, *et al.* Multimodal spinal cord MRI offers accurate diagnostic classification in ALS. *Journal of Neurology, Neurosurgery and Psychiatry*. 2018; 89: 1220–1221.